Eur. J. Mech. A/Solids 18 (1999) 819–835

Parameter identification of gradient enhanced damage models with the finite element method

Rolf Mahnken [a,1], Ellen Kuhl [b,2]

[a] *Institut für Baumechanik und Numerische Mechanik, University of Hannover, Appelstrasse 9a, 30167 Hannover, Germany*
[b] *Institut für Baustatik, University of Stuttgart, Pfaffenwaldring 7, 70550 Stuttgart, Germany*

(Received 12 June 1998; revised and accepted 1 January 1999)

Abstract – In this contribution an algorithm for parameter identification of gradient enhanced damage models is proposed, in which non-uniform distributions of the state variables such as stresses, strains and damage variables are taken into account. To this end a least-squares functional consisting of experimental data and simulated data is minimized, whereby the latter are obtained with the Finite-Element-Method. In order to improve the efficiency of the minimization process, a gradient-based optimization algorithm is applied, and therefore the corresponding sensitivity analysis for the coupled variational problem is described in a systematic manner. For illustrative purpose, the performance of the algorithm is demonstrated for a square panel under tension, in which an isotropic gradient damage model is used. © 1999 Èditions scientifiques et médicales Elsevier SAS

gradient enhanced damage models / parameter identification / sensitivity analysis / optimization / finite element method

1. Introduction

The computational analysis of continuum damage mechanics has been discussed intensively by various researchers during the last decades, see Lemaitre and Chaboche (1990) or Simo and Ju (1987) amongst many others. The damaged material usually exhibits strain softening when loaded above a critical load level. The phenomenon of strain softening might result in localization of deformation in small zones accompanied by the local loss of ellipticity. A well-accepted method to avoid the loss of well-posedness of the governing equations is the introduction of an internal length which governs the width of the localization zone. A numerically elegant way of introducing a length scale has been proposed only recently by Peerlings et al. (1996, 1998) in the context of continuum damage mechanics. This length scale is believed to depend primarily on the microstructure of the material such as the size of the lattice of crystalline materials or the average aggregate size in materials like concrete. However, the internal length scale has only been considered as a mere input parameter hitherto since it cannot be measured directly in an experiment. Furthermore, the determination of the other parameters associated with the continuum damage model is of great interest as well, since they generally cannot be directly related to standard test results (Geers, 1997).

The task of parameter determination based on experimental testing in the mathematical terminology is an inverse problem, see, e.g., Banks and Kunisch (1989), Bui (1994), Bui and Tanaka (1994), Mahnken and Stein (1996). In the classical approach, e.g., a square panel is loaded in compression or tension leading to stress and strain distributions, which are assumed to be uniform within the whole volume of the specimen. However, very often this assumption cannot be verified due to conditions in the laboratory, where, e.g., barreling or necking

[1] E-mail: mahnken@ibnm.uni-hannover.de.
[2] E-mail: kuhl@statik.uni-stuttgart.de.

of the sample takes place, or due to the heterogeneous microstructure of the material giving rise to strain localization.

This contribution aims in a strategy to obtain material parameters where highly non-uniform state variables such as stress, strain and damage variables are taken into account within the domain. To this end the finite element method is used to calculate the associated simulated data of the underlying nonlocal model. In this way also parameter identification based on in-situ experiments becomes possible. This strategy has been applied successfully for parameter identification of material models for inelastic behavior of metals by Mahnken and Stein (1996b, 1997) whereby the experimental data were obtained with an optical method, the "grating method", Andresen et al. (1996).

A least-squares functional is used as an identification criterion, such that the discrepancies between experimental data and simulated data are minimized with respect to a certain norm. For optimization a gradient-based strategy is applied, such as a Quasi-Newton method or a Gauss–Newton method. Therefore the determination of the gradient of the objective function in a *sensitivity analysis* for the coupled variational problem will be described in detail.

An outline of this work is as follows: In Section 2 the constitutive equations of the coupled initial boundary value problem are recalled. In Section 3 the corresponding weak formulation is outlined and Section 4 summarizes the incremental load stepping scheme. Based on the specification of dependent and independent quantities in Section 5, in Section 6 the consistently linearized equations of the weak form and the sensitivity analysis, needed for application of a gradient-based optimization scheme (e.g., Gauss–Newton method, Quasi-Newton method) for parameter identification, are derived. In Section 7 the algorithmic expressions necessary for implementation of a particular geometrically linear enhanced isotropic damage model are presented. Section 8 summarizes some remarks on computational aspects. For illustrative purpose in Section 9 the performance of the algorithm is demonstrated for a square panel under tension, in which the geometrically linear enhanced isotropic damage model of Section 7 is used.

Notations

Square brackets $[\bullet]$ are used throughout the paper to denote 'function of' in order to distinguish from mathematical groupings with parenthesis $(\bullet)$.

2. Strong form of the coupled IBVP

To set the stage we briefly reiterate the coupled initial boundary value problem (IBVP) of a geometrically linear gradient damage model in the framework of continuum mechanics. Following Peerlings et al. (1996) the set of equations is conceptionally split into an equilibrium problem — as a consequence of the balance of linear momentum — and a non-local equivalent strain problem — as a consequence of a Taylor-Series for the non-local equivalent strain variable.

In what follows we define $\mathcal{I} = [t_0, T]$ as the time interval of interest, and $\mathcal{K} = \mathcal{K}_s \times \mathcal{K}_g \subset \mathbb{R}^{n_p}$ denotes the parameter space of material parameters $\boldsymbol{\kappa} = [\boldsymbol{\kappa}_s, \boldsymbol{\kappa}_g]$ for the equilibrium problem and the non-local equivalent strain problem, respectively. Furthermore, $\mathcal{B} \subset \mathbb{E}^{n_{\dim}}$ denotes the configuration occupied by a body $\mathbf{B}$ with placements $\mathbf{x} \in \mathbb{E}^{n_{\dim}}$. Displacements are described by $\mathbf{u}$: $\mathcal{B} \times \mathcal{I} \times \mathcal{K} \mapsto \mathbb{E}^{n_{\dim}}$, and distributed body forces per unit mass are given by the vector field $\mathbf{b}$: $\mathcal{B} \mapsto \mathbb{E}^{n_{\dim}}$ assumed to be independent on time t and material parameters $\boldsymbol{\kappa}$. Additionally $\bar{\varepsilon}_v$: $\mathcal{B} \times \mathcal{I} \times \mathcal{K} \mapsto \mathbb{R}$ defines the non-local equivalent strain, which in the present setting is regarded as an independent field variable. Accordingly, the coupled field equations of the initial boundary value problem read

$$\boxed{\begin{array}{ll} 1. & -\nabla\cdot\boldsymbol{\sigma}=\rho\mathbf{b} \\ 2. & -\nabla\cdot\boldsymbol{\alpha}+\bar{\varepsilon}_v=\varepsilon_v \end{array}} \tag{1}$$

where, for simplicity inertia terms are neglected for the equilibrium problem (1.1), and where ρ denotes the density of the body.

In the above Eq. (1.1), the stress tensor $\boldsymbol{\sigma}$ is obtained from the constitutive equations

$$\boxed{\begin{array}{ll} 1. & \boldsymbol{\sigma}=(1-\zeta)\partial_{\boldsymbol{\varepsilon}}\Psi^s, \quad \text{where} \\ 2. & \boldsymbol{\varepsilon}=\nabla_{\mathbf{x}}^{\text{sym}}\mathbf{u} \\ 3. & \zeta=\zeta[h;\boldsymbol{\kappa}_s] \\ 4. & \Phi=\Phi[\bar{\varepsilon}_v,h] \\ 5. & \Phi\leqslant 0,\ \dot{h}\geqslant 0,\ \Phi\dot{h}=0 \end{array}} \tag{2}$$

In Eq. (2.1) the potential Ψ^s is defined as the quadratic form $\Psi^s = 1/2\ \boldsymbol{\varepsilon}:\mathbf{C}:\boldsymbol{\varepsilon}$, where $\mathbf{C}$ denotes the fourth order elasticity tensor, and Eq. (2.2) expresses the geometrically linear strain displacement relation. (Note, that the material parameters characterizing the elastic behavior are not explicitly mentioned in the above formulation in order to alleviate the notation.) A possible choice for the damage variable $\zeta[h;\boldsymbol{\kappa}_s]$ in Eq. (2.3), which grows from zero to one and which explicitly is dependent on the material parameters $\boldsymbol{\kappa}_s$, is given in the ensuing Section 7. Eq. (2.4) defines a strain-based damage loading function Φ in the sense of Simo and Ju (1987) dependent on a scalar-valued history variable h satisfying a set of discrete loading-unloading conditions (2.5).

The vector $\boldsymbol{\alpha}$ appearing in Eq. (1.2) has the dimension of a length and subsequently will therefore be called *enhanced displacement vector*. Then, in analogy to Eqs (2.1)–(2.2) the constitutive equations for $\boldsymbol{\alpha}$ are

$$\boxed{\begin{array}{ll} 1. & \boldsymbol{\alpha}=\partial_{\boldsymbol{\omega}}\Psi^g[\boldsymbol{\kappa}_g], \quad \text{where} \\ 2. & \boldsymbol{\omega}=\nabla_{\mathbf{x}}\bar{\varepsilon}_v \end{array}} \tag{3}$$

In the simplest case the potential Ψ^g is defined as the quadratic form $\Psi^g = 1/2\ \boldsymbol{\omega}:\mathbf{P}[\boldsymbol{\kappa}_g]:\boldsymbol{\omega}$, where $\mathbf{P}[\boldsymbol{\kappa}_g]$ denotes a second order tensor dependent explicitly on material parameters $\boldsymbol{\kappa}_g$. Note, that the parameters $\boldsymbol{\kappa}_g$ explicitly introduce an internal length scale into the formulation, since they can be interpreted as a weighting coefficient of the strain gradients $\boldsymbol{\omega}$.

Possible choices for the local equivalent strain

$$\boxed{\varepsilon_v=\varepsilon_v[\mathbf{u}]} \tag{4}$$

appearing in (1.2) and depending on the displacement $\mathbf{u}$, are summarized in de Borst et al. (1998), and a particular simple example will be considered in the forthcoming Section 7.

In order to complete the coupled IBVP boundary and initial conditions must be specified: Upon subdividing the boundary $\partial\mathcal{B}$ with outward normal $\mathbf{n}$ into disjoint parts $\partial_u\mathcal{B}\cup\partial_t\mathcal{B}=\partial\mathcal{B}$ with $\partial_u\mathcal{B}\cap\partial_t\mathcal{B}=\emptyset$, Dirichlet boundary conditions $\mathbf{u}=\mathbf{u}^p$ on $\partial\mathcal{B}_u$, Neumann boundary conditions $\boldsymbol{\sigma}\cdot\mathbf{n}=\mathbf{t}^p$ on $\partial\mathcal{B}_t$ and initial conditions $\mathbf{u}=\mathbf{u}^0$, $h=h^0$ in $\mathcal{B}$ at $t=t^0$ are prescribed for the equilibrium problem. Analogously, upon dividing the boundary into disjoint parts $\partial_{\bar{\varepsilon}_v}\mathcal{B}\cup\partial_g\mathcal{B}=\partial\mathcal{B}$ with $\partial_{\bar{\varepsilon}_v}\mathcal{B}\cap\partial_g\mathcal{B}=\emptyset$ Dirichlet boundary conditions $\bar{\varepsilon}_v=\bar{\varepsilon}_v^p$ on $\partial\mathcal{B}_{\bar{\varepsilon}_v}$, Neumann boundary conditions $\boldsymbol{\alpha}\cdot\mathbf{n}=f^p$ on $\partial\mathcal{B}_g$ and initial conditions $\bar{\varepsilon}_v=\bar{\varepsilon}_v^0$ in $\mathcal{B}$ at $t=t^0$ are prescribed for the non-local equivalent strain problem.

3. Weak form of the coupled IBVP

Multiplying the equilibrium equation (1.1) with a test function $\delta\mathbf{u} \in [H_0^1]^{n_{\dim}}$, applying the divergence theorem and taking into account the Neumann boundary condition $\boldsymbol{\sigma} \cdot \mathbf{n} = \mathbf{t}^p$ on $\partial\mathcal{B}_t$ renders the following weak formulation for the equilibrium problem:

$$\begin{aligned}
&1. \quad R_s = G_s^{\text{int}} - G_s^{\text{ext}} = 0 \quad \forall\delta\mathbf{u} \in \left[H_0^1(\mathcal{B})\right]^{n_{\dim}}, \quad \text{where} \\
&2. \quad G_s^{\text{int}} = \int_{\mathcal{B}} \nabla_{\mathbf{x}}\delta\mathbf{u} : \boldsymbol{\sigma} \, \mathrm{d}V \\
&3. \quad G_s^{\text{ext}} = \int_{\mathcal{B}} \rho\delta\mathbf{u} \cdot \mathbf{b} \, \mathrm{d}V + \int_{\partial\mathcal{B}_t} \delta\mathbf{u} \cdot \mathbf{t}^p \, \mathrm{d}A
\end{aligned} \tag{5}$$

and where the stresses $\boldsymbol{\sigma}$ are obtained from the constitutive relations (2).

Analogously the following weak form for the non-local equivalent strain problem is obtained by testing Eq. (1.2) with virtual non-local equivalent strains $\delta\bar{\varepsilon}_v \in [H_0^1(\mathcal{B})]$ and taking into account the Neumann boundary condition $\boldsymbol{\alpha} \cdot \mathbf{n} = f^p$ on $\partial\mathcal{B}_g$:

$$\begin{aligned}
&1. \quad R_g = G_g^{\text{int}} - G_g^{\text{ext}} = 0 \quad \forall\delta\bar{\varepsilon}_v \in H_0^1(\mathcal{B}), \quad \text{where} \\
&2. \quad G_g^{\text{int}} = \int_{\mathcal{B}} (\nabla_{\mathbf{x}}\delta\bar{\varepsilon}_v \cdot \boldsymbol{\alpha} + \delta\bar{\varepsilon}_v\bar{\varepsilon}_v) \, \mathrm{d}V \\
&3. \quad G_g^{\text{ext}} = \int_{\mathcal{B}} \delta\bar{\varepsilon}_v\varepsilon_v \, \mathrm{d}V + \int_{\partial\mathcal{B}_g} \delta\bar{\varepsilon}_v f^p \, \mathrm{d}A
\end{aligned} \tag{6}$$

and where the enhanced displacement vector $\boldsymbol{\alpha}$ is obtained from the constitutive relations (3).

4. Incremental load stepping scheme

The coupled evolution problem (5)–(6) is solved incrementally over a sequence of finite load steps, subsequently labeled by $\Delta t = t^{n+1} - t^n$. On the basis of initial data h^n at each load step the following load stepping algorithm is rendered from the equilibrium problem (5):

$$\begin{aligned}
&1. \quad R_s^{n+1} = G_s^{\text{int},n+1} - G_s^{\text{ext},n+1} = 0 \quad \forall\delta\mathbf{u} \in \left[H_0^1(\mathcal{B})\right]^{n_{\dim}}, \quad \text{where} \\
&2. \quad G_s^{\text{int},n+1} = \int_{\mathcal{B}} \nabla_{\mathbf{x}}\delta\mathbf{u} : \boldsymbol{\sigma}^{n+1} \, \mathrm{d}V \\
&3. \quad G_s^{\text{ext},n+1} = \int_{\mathcal{B}} \rho\delta\mathbf{u} \cdot \mathbf{b} \, \mathrm{d}V + \int_{\partial\mathcal{B}_t} \delta\mathbf{u} \cdot \mathbf{t}_p^{n+1} \, \mathrm{d}A
\end{aligned} \tag{7}$$

and where the stresses $\boldsymbol{\sigma}^{n+1}$ and history variable h^{n+1} are obtained from the discretized set of constitutive equations

$$\begin{aligned}
&1. \quad \boldsymbol{\sigma}^{n+1} = \left(1 - \zeta^{n+1}\right)\partial_{\boldsymbol{\varepsilon}^{n+1}}\Psi^s, \quad \text{where} \\
&2. \quad \boldsymbol{\varepsilon}^{n+1} = \nabla_{\mathbf{x}}^{\text{sym}}\mathbf{u}^{n+1} \\
&3. \quad \zeta^{n+1} = \zeta^{n+1}\left[h^{n+1}; \boldsymbol{\kappa}_s\right] \\
&4. \quad \Phi\left[\bar{\varepsilon}_v^{n+1}, h^{n+1}\right] \leqslant 0, h^{n+1} \geqslant h^n, \quad \Phi\left[\bar{\varepsilon}_v^{n+1}, h^{n+1}\right]\left(h^{n+1} - h^n\right) = 0.
\end{aligned} \tag{8}$$

Analogously the load stepping algorithm for the non-local equivalent strain problem (6) is

$$\begin{aligned}
&1. \quad R_g^{n+1} = G_g^{\text{int},n+1} - G_g^{\text{ext},n+1} = 0 \quad \forall\delta\bar{\varepsilon}_v \in H_0^1(\mathcal{B}), \quad \text{where} \\
&2. \quad G_g^{\text{int},n+1} = \int_{\mathcal{B}} \left(\nabla_{\mathbf{x}}\delta\bar{\varepsilon}_v \cdot \boldsymbol{\alpha}^{n+1} + \delta\bar{\varepsilon}_v\bar{\varepsilon}_v^{n+1}\right) \mathrm{d}V \\
&3. \quad G_g^{\text{ext},n+1} = \int_{\mathcal{B}} \delta\bar{\varepsilon}_v\varepsilon_v^{n+1} \, \mathrm{d}V + \int_{\partial\mathcal{B}_g} \delta\bar{\varepsilon}_v f_p^{n+1} \, \mathrm{d}A
\end{aligned} \tag{9}$$

and where the enhanced displacements $\boldsymbol{\alpha}^{n+1}$ are obtained from the discretized set of constitutive equations

$$\begin{aligned} &1. \quad \boldsymbol{\alpha}^{n+1} = \partial_{\boldsymbol{\omega}^{n+1}} \Psi^g[\boldsymbol{\kappa}_g], \quad \text{where} \\ &2. \quad \boldsymbol{\omega}^{n+1} = \nabla_{\mathbf{x}} \bar{\varepsilon}_v^{n+1}. \end{aligned} \tag{10}$$

5. Specification of dependent and independent quantities

This section aims in a specification of dependent and independent quantities introduced in the previous sections in the framework of a strain driven formulation. This specification will be exploited in the subsequent linearization for the equilibrium iteration and the sensitivity analysis for the identification process.

In view of a strain driven formulation for the stress tensor $\boldsymbol{\sigma}^{n+1}$ and enhanced displacement vector $\boldsymbol{\alpha}^{n+1}$ (typically used in finite element formulations) the following dependencies are observed:

$$\begin{aligned} &1. \quad \boldsymbol{\sigma}^{n+1} = \boldsymbol{\sigma}^{n+1}\big[\boldsymbol{\kappa}_s, h^n, \bar{\varepsilon}_v^{n+1}, \boldsymbol{\varepsilon}^{n+1}[\mathbf{u}^{n+1}]\big] \\ &2. \quad \boldsymbol{\alpha}^{n+1} = \boldsymbol{\alpha}^{n+1}\big[\boldsymbol{\kappa}_g, \boldsymbol{\omega}^{n+1}[\bar{\varepsilon}_v^{n+1}]\big]. \end{aligned} \tag{11}$$

For the ensuing representation it is useful to define a residual $\mathbf{R}$ and a configuration vector $\mathbf{Y}$ as

$$\mathbf{R} =: \begin{bmatrix} R_s \\ R_g \end{bmatrix}, \quad \mathbf{Y} := \begin{bmatrix} \mathbf{u} \\ \bar{\varepsilon}_v \end{bmatrix}. \tag{12}$$

Then the relations (11) reveal the following dependencies for the residual:

$$\mathbf{R}^{n+1} = \hat{\mathbf{R}}^{n+1}\big[\boldsymbol{\kappa}, h^n, \mathbf{Y}^{n+1}\big]. \tag{13}$$

It follows, that for given initial data h^n and given material parameters $\boldsymbol{\kappa}$ the primary unknowns of the coupled problem (7)–(10) within a typical load step are $\mathbf{Y}^{n+1} = [\mathbf{u}^{n+1}, \varepsilon_v^{n+1}]$, and therefore we can formulate the following extended equilibrium problem

$$\boxed{\text{Find } \mathbf{Y}^{n+1}, \text{ such that } \mathbf{R}^{n+1}[\mathbf{Y}^{n+1}] = \mathbf{0}} \tag{14}$$

Furthermore, in order to take into account the complete dependence of $\mathbf{R}^{n+1}$ on the material parameters $\boldsymbol{\kappa}$ we use the fact, that every argument of $\mathbf{R}^{n+1}$ is dependent on $\boldsymbol{\kappa}$. This leads to the representation

$$\mathbf{R}^{n+1} = \hat{\mathbf{R}}^{n+1}\big[\boldsymbol{\kappa}, h^n[\boldsymbol{\kappa}], \mathbf{Y}^{n+1}[\boldsymbol{\kappa}]\big]. \tag{15}$$

6. Associated derivatives of the load discretized weak form

6.1. General concept: Directional derivative and sensitivity operator

Before calculating derivatives of the weak form (13) or (15), respectively, we introduce, motivated by the relation (15), a general (scalar-, vector- or tensor-valued) function

$$\mathbf{w} = \widehat{\mathbf{w}}\big[\boldsymbol{\kappa}, h^n[\boldsymbol{\kappa}], \mathbf{Y}^{n+1}[\boldsymbol{\kappa}]\big] \tag{16}$$

which takes into account the complete dependence of $\mathbf{w}$ on the material parameters $\boldsymbol{\kappa}$. Then the following operators applied to the functional $\widehat{\mathbf{w}}[\boldsymbol{\kappa}, h^n[\boldsymbol{\kappa}], \mathbf{Y}^{n+1}[\boldsymbol{\kappa}]]$ are considered: Firstly, we introduce the standard *directional derivative* (*Gateaux*) *operator*

$$\Delta\widehat{\mathbf{w}} = \frac{\mathrm{d}\widehat{\mathbf{w}}}{\mathrm{d}\mathbf{Y}^{n+1}} \cdot \Delta\mathbf{Y} = \frac{\mathrm{d}}{\mathrm{d}\varepsilon}\big\{\widehat{\mathbf{w}}\big[\boldsymbol{\kappa}, h^n[\boldsymbol{\kappa}], \mathbf{Y}^{n+1}[\boldsymbol{\kappa}] + \varepsilon\Delta\mathbf{Y}\big]\big\}_{\varepsilon=0} \tag{17}$$

necessary for linearization of $\mathbf{w}$. Secondly a *sensitivity operator* is defined

$$\begin{array}{ll} 1. & \partial_{\boldsymbol{\kappa}}\widehat{\mathbf{w}} = \partial^{\varphi}_{\boldsymbol{\kappa}}\widehat{\mathbf{w}} + \partial^{p}_{\boldsymbol{\kappa}}\widehat{\mathbf{w}}, \quad \text{where} \\ 2. & \partial^{\varphi}_{\boldsymbol{\kappa}}\widehat{\mathbf{w}} = \frac{\mathrm{d}\widehat{\mathbf{w}}}{\mathrm{d}\mathbf{Y}^{n+1}} \cdot \partial_{\boldsymbol{\kappa}}\mathbf{Y} = \frac{\mathrm{d}}{\mathrm{d}\varepsilon}\left\{\widehat{\mathbf{w}}\left[\boldsymbol{\kappa}, h^n[\boldsymbol{\kappa}], \mathbf{Y}^{n+1}[\boldsymbol{\kappa}] + \varepsilon\,\partial_{\boldsymbol{\kappa}}\mathbf{Y}\right]\right\}_{\varepsilon=0} \\ 3. & \partial^{p}_{\boldsymbol{\kappa}}\widehat{\mathbf{w}} = \frac{\partial\widehat{\mathbf{w}}}{\partial\boldsymbol{\kappa}} + \frac{\partial\widehat{\mathbf{w}}}{\partial h^n}\frac{\mathrm{d}h^n}{\mathrm{d}\boldsymbol{\kappa}} \end{array} \tag{18}$$

which renders the total derivative $\partial_{\boldsymbol{\kappa}}\mathbf{w} = \mathrm{d}\mathbf{w}/\mathrm{d}\boldsymbol{\kappa}$. Note, that the term $\partial^{\varphi}_{\boldsymbol{\kappa}}\widehat{\mathbf{w}}$ has the same structure as $\Delta\widehat{\mathbf{w}}$ and can thus be obtained from the results for linearization by simply exchanging $\Delta\mathbf{Y}$ with $\partial_{\boldsymbol{\kappa}}\mathbf{Y}$. The second term $\partial^{p}_{\boldsymbol{\kappa}}\widehat{\mathbf{w}}$ essentially excludes the implicit dependence of $\boldsymbol{\kappa}$ via the configuration $\mathbf{Y}^{n+1}$ at the actual time (or load) step t^{n+1} and will subsequently be called *partial parameter derivative*.

6.2. Linearization of the coupled weak form

In view of a Newton algorithm for solving the finite-element discretized counterpart of the equilibrium problem (14) a linearization of the residual $\mathbf{R}^{n+1}$ with respect to the configuration vector $\mathbf{Y}^{n+1}$ becomes necessary. Application of the formula for the directional derivative (17) to the residual $\mathbf{R}^{n+1}$ renders the following result:

$$\Delta_Y\widehat{\mathbf{R}}^{n+1} = \partial_{\mathbf{Y}}\widehat{\mathbf{R}}^{n+1} \cdot \Delta\mathbf{Y} = \begin{bmatrix} \Delta_Y G_s^{\mathrm{int},n+1} - \Delta_Y G_s^{\mathrm{ext},n+1} \\ \Delta_Y G_g^{\mathrm{int},n+1} - \Delta_Y G_g^{\mathrm{ext},n+1} \end{bmatrix}, \tag{19}$$

where

$$\begin{array}{ll} 1. & \Delta_Y G_s^{\mathrm{int},n+1} = \Delta_u G_s^{\mathrm{int},n+1} + \Delta_{\bar{\varepsilon}_v} G_s^{\mathrm{int},n+1} \\ 2. & \Delta_u G_s^{\mathrm{int},n+1} = \int_{\mathcal{B}} \nabla_{\mathbf{x}}\delta\mathbf{u} : \mathbf{C}^{n+1} : \nabla_{\mathbf{x}}\Delta\mathbf{u}\ \mathrm{d}V \\ 3. & \Delta_{\bar{\varepsilon}_v} G_s^{\mathrm{int},n+1} = \int_{\mathcal{B}} \nabla_{\mathbf{x}}\delta\mathbf{u} : \partial_{\bar{\varepsilon}_v^{n+1}}\boldsymbol{\sigma}^{n+1}\Delta\bar{\varepsilon}_v\ \mathrm{d}V \\ 4. & \Delta_Y G_s^{\mathrm{ext},n+1} = 0 \end{array} \tag{20}$$

and

$$\begin{array}{ll} 1. & \Delta_Y G_g^{\mathrm{int},n+1} = \Delta_u G_g^{\mathrm{int},n+1} + \Delta_{\bar{\varepsilon}_v} G_g^{\mathrm{int},n+1} \\ 2. & \Delta_u G_g^{\mathrm{int},n+1} = 0 \\ 3. & \Delta_{\bar{\varepsilon}_v} G_g^{\mathrm{int},n+1} = \int_{\mathcal{B}} \nabla_{\mathbf{x}}\delta\bar{\varepsilon}_v \cdot \mathbf{P} \cdot \nabla_{\mathbf{x}}\Delta\bar{\varepsilon}_v\ \mathrm{d}V \\ 4. & \Delta_Y G_g^{\mathrm{ext},n+1} = \Delta_u G_g^{\mathrm{ext},n+1} + \Delta_{\bar{\varepsilon}_v} G_g^{\mathrm{ext},n+1} \\ 5. & \Delta_u G_g^{\mathrm{ext},n+1} = \int_{\mathcal{B}} \delta\bar{\varepsilon}_v \partial_{\boldsymbol{\varepsilon}^{n+1}}\varepsilon_v^{n+1} : \nabla_{\mathbf{x}}\Delta\mathbf{u}\ \mathrm{d}V \\ 6. & \Delta_{\bar{\varepsilon}_v} G_g^{\mathrm{ext},n+1} = 0. \end{array} \tag{21}$$

Thus it remains to determine the consistent moduli

$$\mathbf{C}^{n+1} = \partial_{\boldsymbol{\varepsilon}^{n+1}}\boldsymbol{\sigma}^{n+1}, \quad \partial_{\bar{\varepsilon}_v^{n+1}}\boldsymbol{\sigma}^{n+1}, \quad \partial_{\boldsymbol{\varepsilon}^{n+1}}\varepsilon_v^{n+1}, \quad \mathbf{P}. \tag{22}$$

For a specific example of a gradient enhanced damage model these will be derived in the forthcoming Section 7.3.

6.3. Sensitivity analysis for the coupled weak form

In view of a gradient based optimization algorithm for solving a least-squares optimization problem for parameter identification a sensitivity analysis of the residual $\widehat{\mathbf{R}}$ — *at equilibrium* — with respect to the material

parameters becomes necessary. In order to perform the sensitivity analysis at the actual time step it is assumed, that the sensitivities $\partial_{\boldsymbol{\kappa}} h^n$ evaluated at the previous load step t^n are given. Upon using the representation (15) for the residual its complete sensitivity is given according to the sensitivity operator (18) as

$$\partial_{\boldsymbol{\kappa}} \widehat{\mathbf{R}}^{n+1} = \partial_{\mathbf{Y}} \widehat{\mathbf{R}}^{n+1} \cdot \partial_{\boldsymbol{\kappa}} \mathbf{Y} + \partial_{\boldsymbol{\kappa}}^{p} \widehat{\mathbf{R}}^{n+1} = \mathbf{0}. \tag{23}$$

Since the first part on the right-hand side has the same structure as the directional derivative (19), where $\Delta\mathbf{Y}$ is replaced by $\partial_{\boldsymbol{\kappa}}\mathbf{Y}$, the results of the linearization procedure of Section 6.2 can be directly exploited in order to determine this part. The second part of the right-hand side in Eq. (23) is defined according to the partial sensitivity operator (18.3). Then the relation (23) defines a linear equation for $\partial_{\boldsymbol{\kappa}}\mathbf{Y}$. In the practical implementation this is obtained by calculating $\partial_{\boldsymbol{\kappa}}^{p}\widehat{\mathbf{R}}$ in a *pre-processing* step, and then solve Eq. (23) for $\partial_{\boldsymbol{\kappa}}\mathbf{Y}$ (with consistent tangent matrix already factorized in the equilibrium iteration). Furthermore, the complete sensitivity of the quantity h^{n+1}, which is dependent on $\mathbf{Y}^{n+1}$, is calculated in a *post-processing* step, see Mahnken and Stein (1996b, 1997)

6.3.1. *Pre-processing step*

It has already been mentioned, that the second part of the right-hand side in Eq. (23.3) is obtained by use of the partial sensitivity operator (18.3). Accordingly the following result is obtained:

$$\partial_{\boldsymbol{\kappa}}^{p} \widehat{\mathbf{R}}^{n+1} = \begin{bmatrix} \partial_{\boldsymbol{\kappa}}^{p} G_s^{\mathrm{int},n+1} - \partial_{\boldsymbol{\kappa}}^{p} G_s^{\mathrm{ext},n+1} \\ \partial_{\boldsymbol{\kappa}}^{p} G_g^{\mathrm{int},n+1} - \partial_{\boldsymbol{\kappa}}^{p} G_g^{\mathrm{ext},n+1} \end{bmatrix}, \tag{24}$$

where

$$\begin{aligned} &1. \quad \partial_{\boldsymbol{\kappa}}^{p} G_s^{\mathrm{int},n+1} = \textstyle\int_{\mathcal{B}} \nabla_{\mathbf{x}} \delta\mathbf{u} : \partial_{\boldsymbol{\kappa}}^{p} \boldsymbol{\sigma}^{n+1} \, \mathrm{d}V \\ &2. \quad \partial_{\boldsymbol{\kappa}}^{p} G_s^{\mathrm{ext},n+1} = 0 \end{aligned} \tag{25}$$

and

$$\begin{aligned} &1. \quad \partial_{\boldsymbol{\kappa}}^{p} G_g^{\mathrm{int},n+1} = \textstyle\int_{\mathcal{B}} \nabla_{\mathbf{x}} \delta\bar{\varepsilon}_v \cdot \partial_{\boldsymbol{\kappa}}^{p} \boldsymbol{\alpha}^{n+1} \, \mathrm{d}V \\ &2. \quad \partial_{\boldsymbol{\kappa}}^{p} G_g^{\mathrm{ext},n+1} = 0. \end{aligned} \tag{26}$$

In the above equations, according to the partial sensitivity operator (18.3), we have made use of the relations

$$\begin{aligned} &1. \quad \partial_{\boldsymbol{\kappa}}^{p} \boldsymbol{\varepsilon}^{n+1} = \partial_{\boldsymbol{\kappa}}^{p} \nabla_{\mathbf{x}} \mathbf{u}^{n+1} = 0 \\ &2. \quad \partial_{\boldsymbol{\kappa}}^{p} \bar{\varepsilon}_v^{n+1} = 0 \end{aligned} \tag{27}$$

in deriving (26.1) and (26.2), respectively. Thus it remains to determine the partial parameter derivatives $\partial_{\boldsymbol{\kappa}}^{p}\boldsymbol{\sigma}^{n+1}$ and $\partial_{\boldsymbol{\kappa}}^{p}\boldsymbol{\alpha}^{n+1}$ depending on the specific constitutive equations for the equilibrium problem and the non-local equivalent strain problem, respectively.

6.3.2. *Post-processing step*

The fact, that $\boldsymbol{\sigma}^{n+1}$ is also dependent on the history variable h^n (see Eq. (11.1)), entails a dependence of $\partial_{\boldsymbol{\kappa}}^{p}\boldsymbol{\sigma}^{n+1}$ on the parameter sensitivity of the history variable $\partial_{\boldsymbol{\kappa}} h^n$. Therefore, having solved Eq. (23) for $\partial_{\boldsymbol{\kappa}}\mathbf{Y}^{n+1}$ with $\partial_{\mathbf{Y}}\widehat{\mathbf{R}}^{n+1}$ and $\partial_{\boldsymbol{\kappa}}^{p}\widehat{\mathbf{R}}^{n+1}$ derived as explained in Sections 6.2 and 6.3.1, respectively, it becomes necessary to calculate the quantity $\partial_{\boldsymbol{\kappa}} h^{n+1}$ to make it available for determination of sensitivities in the next load step. For a specific isotropic damage model this is described in the ensuing Section 7.

Table I. Geometrically linear gradient enhanced damage model.

Isotropic linear elastic stress–strain relation
$$\boldsymbol{\sigma} = (1-\zeta)\mathbf{C}:\boldsymbol{\varepsilon} = (1-\zeta)(2G\,\mathrm{dev}\,\boldsymbol{\varepsilon} + K\,\mathrm{tr}\,\boldsymbol{\varepsilon}\mathbf{1})$$
Strain-based damage loading function
$$\Phi = \Phi[\bar{\varepsilon}_v, h] = \bar{\varepsilon}_v - h$$
Local equivalent strain
$$\varepsilon_v = \sqrt{\frac{1}{E}\boldsymbol{\varepsilon}:\mathbf{C}:\boldsymbol{\varepsilon}}$$
Exponential softening relation
$$\zeta(h) = \begin{cases} 0 & \text{if } h < \kappa, \\ 1 - \frac{\kappa}{h}\left[1 - \alpha + \alpha\exp(-\eta(h-\kappa))\right] & \text{if } h \geqslant \kappa \end{cases}$$
Evolution
$$\dot{h} = \begin{cases} 0 & \text{if } \dot{\bar{\varepsilon}} < 0, \\ \dot{\bar{\varepsilon}} & \text{if } \dot{\bar{\varepsilon}} \geqslant 0 \end{cases}$$
Loading and unloading conditions
$$\Phi \leqslant 0, \qquad \dot{h} \geqslant 0, \qquad \dot{h}\Phi = 0$$
Isotropic linear enhanced constitutive relation
$$\boldsymbol{\alpha} = c\,\boldsymbol{\omega}$$
Material parameters
$$\boldsymbol{\kappa}_s = [\kappa, \alpha, \eta], \quad \boldsymbol{\kappa}_g = [c]$$

7. A particular gradient enhanced damage model

7.1. Constitutive relations

The constitutive relations of a gradient enhanced isotropic damage model in the framework of a geometric linear theory are summarized in *table I*: Here, an isotropic linear elastic stress strain relation and a strain-based damage loading function Φ are specified. Furthermore a simple choice for the local equivalent strain ε_v is assumed. More detailed formulations, which, e.g., take into account different tensile and compression mechanisms are discussed in de Borst et al. (1998). The extension of the proposed method to more enhanced models like the microplane model proposed by Kuhl et al. is straightforward. Furthermore, in *table I*, an exponential softening relation is specified and the loading and unloading conditions for derivation of the history variable h are recalled. Next, the isotropic linear enhanced constitutive relation is given, and finally the material parameters characterizing the material are summarized.

7.2. Stress update algorithm

Using standard notation we assume that for a load increment $\Delta t = t^{n+1} - t^n$ the strains $\boldsymbol{\varepsilon}^{n+1} = \nabla_{\mathbf{x}}^{\mathrm{sym}}\mathbf{u}^{n+1}$, the equivalent strain gradient $\boldsymbol{\omega}^{n+1} = \nabla_{\mathbf{x}}\varepsilon_v^{n+1}$ and an initial value for the history variable h^n within a strain driven

algorithm are given. Then, according to the relations (8) the stress tensor $\boldsymbol{\sigma}^{n+1}$ and the history variable h^{n+1} at load step t^{n+1} are obtained as

$$\begin{aligned}
&1.\quad \boldsymbol{\sigma}^{n+1} = \left(1-\zeta^{n+1}\right)\mathbf{C}:\boldsymbol{\varepsilon}^{n+1}\\
&2.\quad h^{n+1} = \begin{cases} h^n & \text{if } \bar{\varepsilon}_v^{n+1} < h^n \\ \bar{\varepsilon}_v^{n+1} & \text{if } \bar{\varepsilon}_v^{n+1} \geqslant h^n \end{cases}\\
&3.\quad \zeta^{n+1} = 1 - \tfrac{\kappa}{h^{n+1}}\left[1-\alpha+\alpha\exp\left(-\eta\left(h^{n+1}-\kappa\right)\right)\right].
\end{aligned} \tag{28}$$

Analogously, according to (10) the enhanced displacements are updated as

$$\boldsymbol{\alpha}^{n+1} = c\boldsymbol{\omega}^{n+1}. \tag{29}$$

7.3. Consistent tangent moduli

The consistent tangent moduli (22) are obtained by straightforward differentiation with the following results:

$$\mathbf{C}^{n+1} = \partial_{\boldsymbol{\varepsilon}^{n+1}}\boldsymbol{\sigma}^{n+1} = \left(1-\zeta^{n+1}\right)\mathbf{C}, \tag{30}$$

$$\partial_{\bar{\varepsilon}_v^{n+1}}\boldsymbol{\sigma}^{n+1} = -\partial_{\bar{\varepsilon}_v^{n+1}}\zeta^{n+1}\mathbf{C}:\boldsymbol{\varepsilon}, \tag{31}$$

where

$$\partial_{\bar{\varepsilon}_v^{n+1}}\zeta^{n+1} = \begin{cases} 0 & \text{if } \bar{\varepsilon}_v^{n+1} < h^n, \\ \frac{\kappa}{(h^{n+1})^2}\left(1-\alpha+\alpha\exp\left(-\eta\left(h^{n+1}-\kappa\right)\right)\right) + \frac{\kappa}{h^{n+1}}\eta\alpha\exp\left(-\eta\left(h^{n+1}-\kappa\right)\right) & \text{if } \bar{\varepsilon}_v^{n+1} \geqslant h^n, \end{cases} \tag{32}$$

$$\partial_{\boldsymbol{\varepsilon}^{n+1}}\varepsilon_v^{n+1} = \frac{1}{E\varepsilon_v^{n+1}}\mathbf{C}:\boldsymbol{\varepsilon}^{n+1}, \tag{33}$$

$$\mathbf{P} = \operatorname{diag}\{c\}. \tag{34}$$

7.4. Sensitivity analysis

This section is concerned with determination of $\partial_{\boldsymbol{\kappa}}^p\boldsymbol{\sigma}^{n+1}$ and $\partial_{\boldsymbol{\kappa}}^p\boldsymbol{\alpha}^{n+1}$ appearing in Eq. (25.1) and Eq. (26.1) at the actual load step t^{n+1} in a *pre-processing* step. Therefore it is assumed, that the sensitivities $\partial_{\boldsymbol{\kappa}}h^n$ are given, evaluated at the previous load step t^n in a *post-processing* step. However, beforehand some prerequisite results are obtained.

7.4.1. Sensitivity of the stress tensor and the history variable

From the relations (28) the total sensitivity for stress tensor is derived as

$$\partial_{\boldsymbol{\kappa}}\boldsymbol{\sigma}^{n+1} = \left(1-\zeta^{n+1}\right)\mathbf{C}:\partial_{\boldsymbol{\kappa}}\boldsymbol{\varepsilon}^{n+1} - \partial_{\boldsymbol{\kappa}}\zeta^{n+1}\mathbf{C}:\boldsymbol{\varepsilon}^{n+1} \tag{35}$$

and where $\partial_{\boldsymbol{\kappa}}\boldsymbol{\varepsilon}^{n+1} = \partial_{\boldsymbol{\kappa}}\nabla_{\mathbf{x}}^{\text{sym}}\mathbf{u}^{n+1}$.

According to the stress update formula (28.2) the sensitivity of the history variable is:

$$\partial_{\boldsymbol{\kappa}}h^{n+1} = \begin{cases} \partial_{\boldsymbol{\kappa}}h^n & \text{if } \bar{\varepsilon}_v^{n+1} < h^n, \\ \partial_{\boldsymbol{\kappa}}\bar{\varepsilon}_v^{n+1} & \text{if } \bar{\varepsilon}_v^{n+1} \geqslant h^n. \end{cases} \tag{36}$$

Then, from the update formula (28.3) the sensitivity of the damage variable is:

$$\partial_{\boldsymbol{\kappa}}\zeta^{n+1} = \partial_{h^{n+1}}\zeta^{n+1}\partial_{\boldsymbol{\kappa}}h^{n+1} + \frac{\partial\zeta^{n+1}}{\partial\boldsymbol{\kappa}} \tag{37}$$

and where with arrangement from *table I*

$$\frac{\partial \zeta^{n+1}}{\partial \boldsymbol{\kappa}} = \begin{bmatrix} -\frac{1}{h^{n+1}}\left(1-\alpha+\alpha\exp\left(-\eta\left(h^{n+1}-\kappa\right)\right)\right) - \frac{\kappa}{h^{n+1}}\eta\alpha\exp\left(-\eta\left(h^{n+1}-\kappa\right)\right) \\ -\frac{\kappa}{h^{n+1}}\left(-1+\exp\left(-\eta\left(h^{n+1}-\kappa\right)\right)\right) \\ \frac{\kappa}{h^{n+1}}\alpha\exp\left(-\eta\left(h^{n+1}-\kappa\right)\right)\left(h^{n+1}-\kappa\right) \\ 0 \end{bmatrix}. \tag{38}$$

7.4.2. Pre-processing step: Partial parameter sensitivity of the stresses

With the relations of the previous section the final result for the partial parameter sensitivity of the stresses $\partial^p_{\boldsymbol{\kappa}}\boldsymbol{\sigma}^{n+1}$ is obtained from Eqs (35)–(38), by excluding derivatives with respect to $\boldsymbol{\kappa}$ via the configuration vector $\mathbf{Y}$ according to the sensitivity operator (18). The resulting expressions of this pre-processing step are summarized in *table II*.

Accordingly the partial parameter sensitivity of the enhanced displacement vector $\partial^p_{\boldsymbol{\kappa}}\boldsymbol{\alpha}^{n+1}$ is obtained from Eq. (29)

$$\partial^p_{\boldsymbol{\kappa}}\boldsymbol{\alpha}^{n+1} = \boldsymbol{\omega}^{n+1} \otimes \partial^p_{\boldsymbol{\kappa}} c \tag{39}$$

and where with arrangement from *table I*

$$\partial^p_{\boldsymbol{\kappa}} c = \begin{bmatrix} 0 \\ 0 \\ 0 \\ 1 \end{bmatrix}. \tag{40}$$

7.4.3. Post-processing step: Sensitivity of the history variables

From the pre-processing step in *table II* it can be seen, that the partial sensitivity $\partial^p_{\boldsymbol{\kappa}}\boldsymbol{\sigma}^{n+1}$ at the actual load step is calculated by use of the quantities $\partial_{\boldsymbol{\kappa}} h^n$ from the previous load step. In the practical implementation this is realized by calculation of $\partial_{\boldsymbol{\kappa}} h^{n+1}$ at the actual load step to make it available for the ensuing load step. The final results of this post-processing step are also summarized in *table II*.

8. Remarks on computational aspects

1. The continuum equations of Section 4 to Section 6 are amenable for spatial discretization. An extensive description for the implementation is given by Peerlings et al. (1996), and therefore we will not elaborate on this issue. Special care must be taken for the different interpolation orders for the displacement and the non-local equivalent strain. To this end, the simplest combinations of C^0 continuous displacement and non-local equivalent strain expansions giving balanced approximations of the two different fields are either triangular P2/P1 or quadrilateral Q2/Q1 elements.
2. For parameter identification of the coupled model it is assumed, that experimental data for the displacements $\widetilde{\mathbf{u}}^{n+1} \in \mathbb{R}^{mps} \times \mathbb{R}^{n_{\dim}}$, $n = 0, \ldots, N-1$ are given, where mps denote the associated number of observation points, and $\{t^j\}_{j=1}^{n_{tdat}}$ denote the observation states. If, for ease of notation we assume that the latter are identical to the load steps $\{t^n\}_{n=1}^{N}$, a typical least-squares problem for parameter identification has the following structure

$$\boxed{\text{Find } \boldsymbol{\kappa} \in \mathcal{K} : f[\boldsymbol{\kappa}] := \tfrac{1}{2}\sum_{n=0}^{N-1} ||\mathbf{u}^{n+1}[\boldsymbol{\kappa}] - \widetilde{\mathbf{u}}^{n+1}||^2 \longrightarrow \min_{\boldsymbol{\kappa}}} \tag{41}$$

Table II. Geometrically linear gradient enhanced damage model: Partial parameter sensitivity of stresses for pre-processing step and parameter sensitivity of history variable for post processing step.

Partial parameter sensitivity for stresses (pre-processing)

Input: $\partial_{\boldsymbol{\kappa}} h^n$

- History variable

$$\partial_{\boldsymbol{\kappa}}^p h^{n+1} = \begin{cases} \partial_{\boldsymbol{\kappa}} h^n & \text{if } \bar{\varepsilon}_v^{n+1} < h^n, \\ \mathbf{0} & \text{if } \bar{\varepsilon}_v^{n+1} \geqslant h^n \end{cases}$$

- Damage variable

$$\partial_{\boldsymbol{\kappa}}^p \zeta^{n+1} = \partial_{h^{n+1}} \zeta^{n+1} \partial_{\boldsymbol{\kappa}}^p h^{n+1} + \frac{\partial \zeta^{n+1}}{\partial \boldsymbol{\kappa}},$$

where

$$\partial_{h^{n+1}} \zeta^{n+1} = \frac{\kappa}{(h^{n+1})^2} \left(1 - \alpha + \alpha \exp\left(-\eta \left(h^{n+1} - \kappa\right)\right)\right) + \frac{\kappa}{h^{n+1}} \eta\alpha \exp\left(-\eta \left(h^{n+1} - \kappa\right)\right)$$

and

$$\frac{\partial \zeta^{n+1}}{\partial \boldsymbol{\kappa}} = \begin{bmatrix} -\frac{1}{h^{n+1}} \left(1 - \alpha + \alpha \exp\left(-\eta \left(h^{n+1} - \kappa\right)\right)\right) - \frac{\kappa}{h^{n+1}} \eta\alpha \exp\left(-\eta \left(h^{n+1} - \kappa\right)\right) \\ -\frac{\kappa}{h^{n+1}} \left(-1 + \exp\left(-\eta \left(h^{n+1} - \kappa\right)\right)\right) \\ \frac{\kappa}{h^{n+1}} \alpha \exp\left(-\eta \left(h^{n+1} - \kappa\right)\right) (h^{n+1} - \kappa) \\ 0 \end{bmatrix}$$

- Stress tensor

$$\partial_{\boldsymbol{\kappa}}^p \boldsymbol{\sigma}^{n+1} = -\partial_{\boldsymbol{\kappa}}^p \zeta^{n+1} \mathbf{C} : \boldsymbol{\varepsilon}$$

- Enhanced displacement vector

$$\partial_{\boldsymbol{\kappa}}^p \boldsymbol{\alpha}^{n+1} = \boldsymbol{\omega}^{n+1} \otimes \partial_{\boldsymbol{\kappa}}^p c,$$

where

$$\partial_{\boldsymbol{\kappa}}^p c = \begin{bmatrix} 0 \\ 0 \\ 0 \\ 1 \end{bmatrix}$$

Parameter sensitivity of history variable (post-processing)

Input: $\partial_{\boldsymbol{\kappa}} h^n$, $\partial_{\boldsymbol{\kappa}} \bar{\varepsilon}_v^{n+1}$

$$\partial_{\boldsymbol{\kappa}} h^{n+1} = \begin{cases} \partial_{\boldsymbol{\kappa}} h^n & \text{if } \bar{\varepsilon}_v^{n+1} < h^n, \\ \partial_{\boldsymbol{\kappa}} \bar{\varepsilon}_v^{n+1} & \text{if } \bar{\varepsilon}_v^{n+1} \geqslant h^n \end{cases}$$

where $\| \bullet \|$ denotes a norm for vectors. Alternatively, a weighted least-squares functional based on the maximum-likelihood method can be used as an objective function, see, e.g., Mahnken (1998).

3. Concerning the gradient based optimization strategy for solution of problem (41), here only some basic ideas shall be presented. More details pertaining to mathematical issues can be found in Luenberger (1984), Dennis and Schnabel (1983), Bertsekas (1982), Mahnken (1992).
   In the present setting a projection algorithm due to Bertsekas (1982) with iteration scheme

$$\boldsymbol{\kappa}^{(j+1)} = \mathcal{P}\left\{\boldsymbol{\kappa}^{(j)} - \alpha^{(j)} \mathbf{H}^{(j)} \nabla f\left(\boldsymbol{\kappa}^{(j)}\right)\right\}, \quad j = 0, 1, 2, \ldots, \tag{42}$$

is proposed. The projection operator $\mathcal{P}$ is introduced, in order to take into account lower and upper bounds $a_i, b_i, i = 1, \ldots, n_p$, for the material parameters and is defined as

$$\mathcal{P}\{\boldsymbol{\kappa}\}_i := \min\big(\max(a_i, \kappa_i), b_i\big), \quad i = 1, \ldots, n_p. \tag{43}$$

Furthermore, $\alpha^{(j)}$ is a step-length determined in a line search, which may be based on function evaluations (e.g., Armijo line-search). The iteration matrix $\mathbf{H}^{(j)}$ is a positive-definite iteration matrix such as the inverse of the Gauss–Newton matrix or a BFGS matrix, which in the context of the above iteration scheme has to be "diagonalized" (see Bertsekas (1982) for an explanation of this terminology), in order to ensure descent properties of the iteration scheme. Concerning the specific update formula for $\mathbf{H}_{BFGS}$, we refer to Dennis and Schnabel (1983) and to the modification due to Powell (1977) in order to preserve positive-definiteness (see also Luenberger (1984), p. 448). Lastly we remark, that the inverse of the Hessian is not recommended as an iteration matrix, since (i) it requires second order derivatives and (ii) positive definiteness is not guaranteed during the iteration process.

4. The main practical consequence of the recursion structure for history dependent problems obtained by the sensitivity analysis is, that determination of $\partial_{\boldsymbol{\kappa}}\mathbf{Y}^{n+1}$ is performed *simultaneously* to the step-by-step solution of the direct problem. In this respect, when solving the direct problem for a given set of parameters $\boldsymbol{\kappa}^{(j)}$, three additional steps are necessary at the converged state of each load step: Firstly a partial load vector, which basically is a discretized form of the partial parameter derivative of the residual $\partial^p_{\boldsymbol{\kappa}}\mathbf{R}^{n+1}$ is determined in a pre-processing procedure. Secondly, a linear system is solved with a tangent matrix already factorized at the converged state of the solution procedure for the direct problem. Thirdly, in a post-processing procedure an update of the total derivative of internal strain variables $\partial_{\boldsymbol{\kappa}} h^{n+1}$ is performed at each quadrature point (in addition to the standard update procedure of internal strain-like variables h^{n+1}).
5. A reduction of the execution time is obtained, by exploiting the Armijo line-search in the iteration scheme. In this respect the actual value $\hat{f}^{n+1}(\boldsymbol{\kappa}^{(j+1)}(\alpha))$ is compared with the final value $f(\boldsymbol{\kappa}^{(j)})$ of the previous iteration step *after each load step* $n+1$ *during the incremental solution procedure*. If $\hat{f}^{n+1}(\boldsymbol{\kappa}^{(j+1)}(\alpha)) > f(\boldsymbol{\kappa}^{(j)})$ for some load step $n+1$, the inner iteration for solution of the direct problem is interrupted, and a new $\boldsymbol{\kappa}^{(j+1)}(\alpha)$ is generated by a line-search backtracking step. This strategy avoids the costly finishing of the solution for direct problems with inadequate parameters $\boldsymbol{\kappa}^{(j+1)}(\alpha)$.

9. Square panel under tension

This example intends to test our optimization algorithm based on synthetic data, where a square panel under tension is considered. The panel is assumed to obey a geometrically linear enhanced isotropic damage model with an isotropic softening rule as summarized in *table I.*

Conceptionally we proceed as follows: Firstly a coupled (direct) problem is solved with the following assumed material data: $E = 20000$ for Youngs modulus, $\nu = 0.2$ for Poissons ratio, $\kappa = 0.0001$, $\alpha = 0.96$, $\eta = 350$, $c = 5$ (note, that units are not given for material constants, loading and geometry for this purely numerical example). Q2/Q1-elements are used in the finite element implementation. The load is applied displacement controlled in 300 load steps with unequal size.

The resulting contour plot for the damage variable at the end of the load history is depicted in *figure 2*. The localization of the deformation in a zone of the width of one element is obviously avoided because of the introduction of strain gradients in the damage loading function. In *figure 3* the von Mises stress versus the vertical top displacement is shown for two corner points of the specimen, thus reflecting the non-uniformness within the structure.

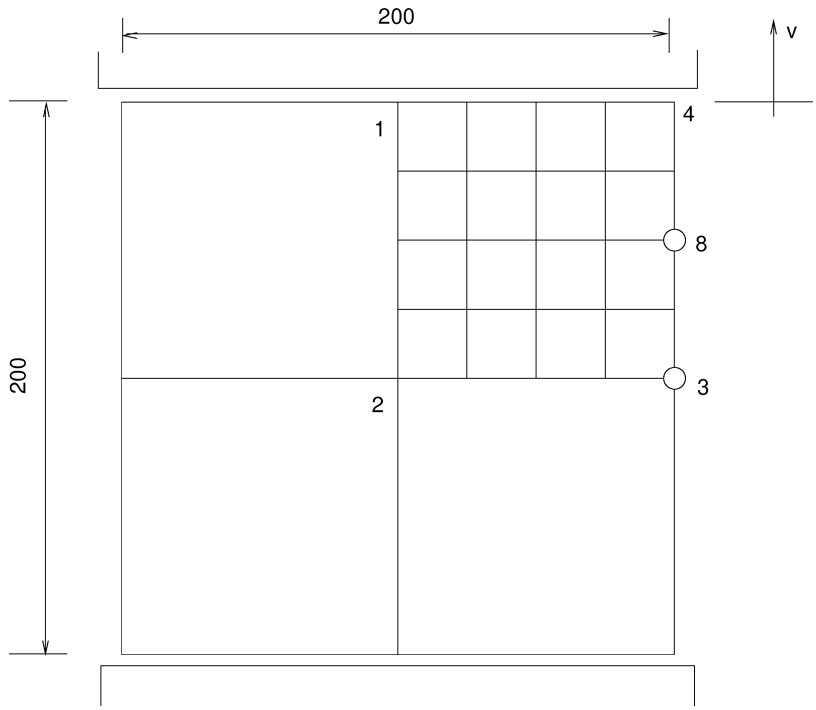

Figure 1. Square panel under tension: Geometry, discretization and position of fictitious observations points represented by circles.

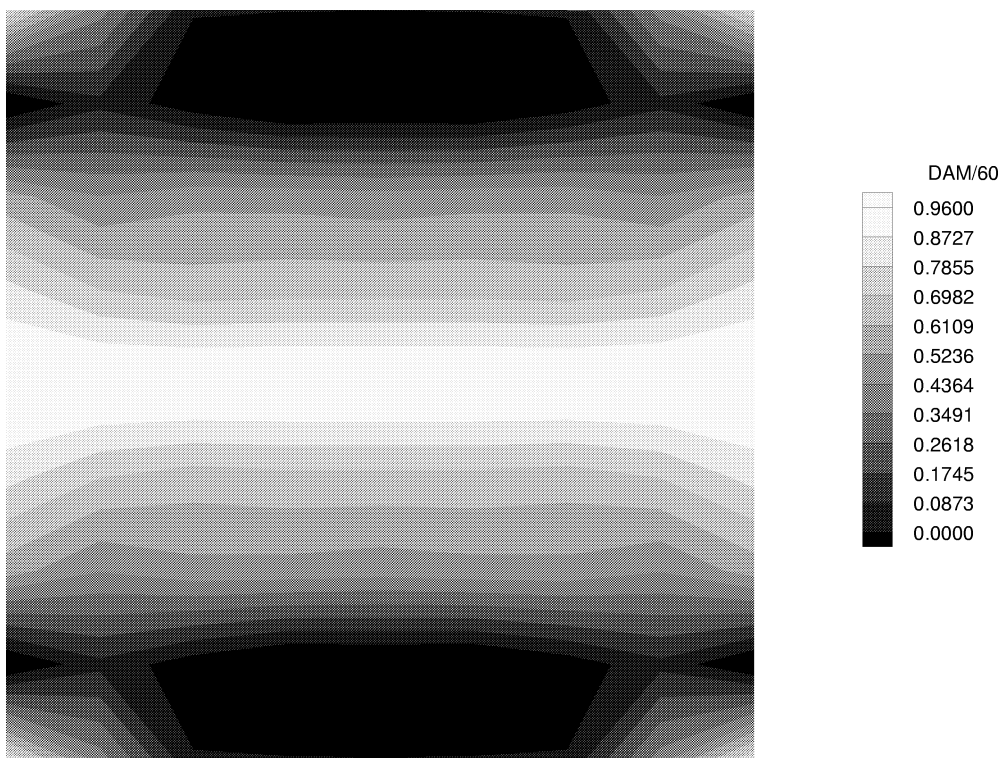

Figure 2. Square panel under tension: Contour plot for the damage variable at the end of loading.

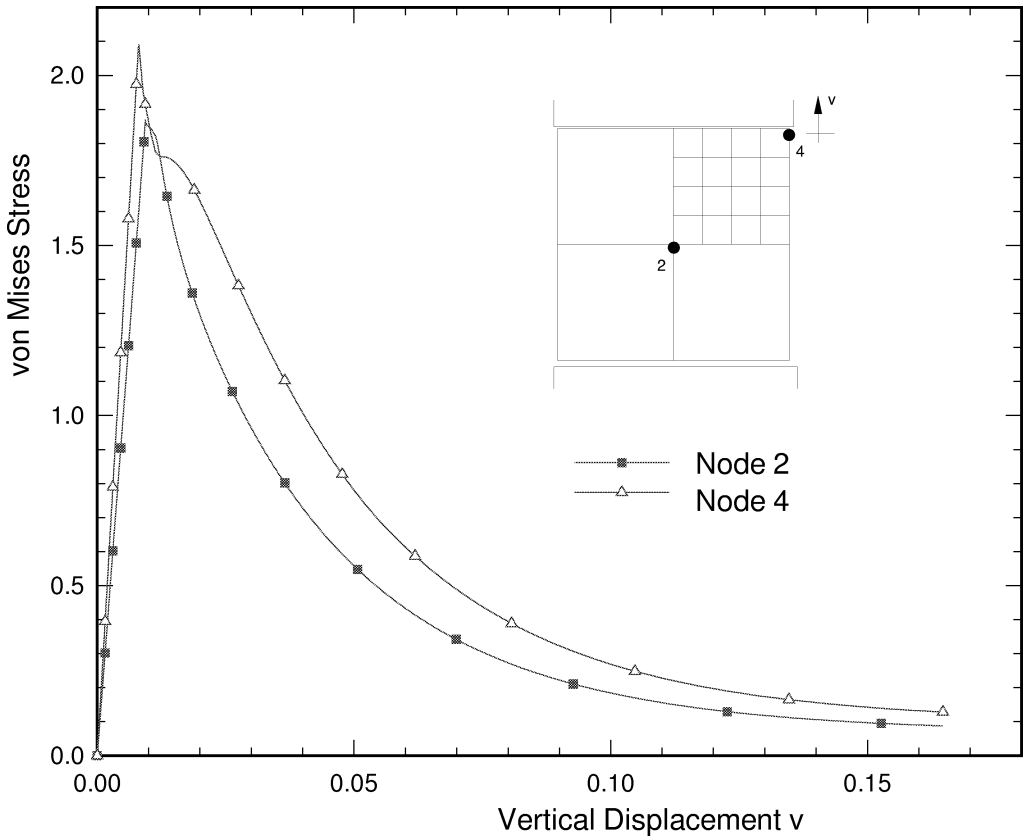

Figure 3. Square panel under tension: von Mises stress versus vertical top displacement at two different points of the sample.

The results for the horizontal displacements u_3^n, at node number 3 and for the horizontal and vertical displacements u_8^n, v_8^n at node number 8 marked in *figure 1* are recorded at n_{tdat} = 60 load steps $n = 5, 10, 15, \ldots$ and used as synthetic data in order to test our optimization algorithm.

In the optimization process, it is the object to re-obtain the target parameters α, η, c which are summarized in the third column of *table III*. As an objective function the following scaled least-squares function is considered

$$f[\boldsymbol{\kappa}] = \sum_{n \in I} \left(\frac{u_3^n[\boldsymbol{\kappa}] - \widetilde{u}_3^n}{u_3^n[\boldsymbol{\kappa}]^{(j=0)} - \widetilde{u}_3^n} \right)^2 + \left(\frac{u_8^n[\boldsymbol{\kappa}] - \widetilde{u}_8^n}{u_8^n[\boldsymbol{\kappa}]^{(j=0)} - \widetilde{u}_8^n} \right)^2 + \left(\frac{v_8^n[\boldsymbol{\kappa}] - \widetilde{v}_8^n}{v_8^n[\boldsymbol{\kappa}]^{(j=0)} - \widetilde{v}_8^n} \right)^2 \longrightarrow \min_{\boldsymbol{\kappa}}, \tag{44}$$

where $I = [5, 10, 15, \ldots]$. The upper index $(\bullet)^{(j)}$ refers to the iteration number of the projection algorithm (42) due to Bertsekas (1982), where a BFGS update formula is used to calculate the iteration matrix $\mathbf{H}^{(j)}$. The starting vector for the optimization process is given in the second column of *table III*. From the fourth column of *table III* it can be observed, that at the solution point all 3 parameters of the coupled problem are re-obtained exactly.

In *figure 4* the scaled objective function (44) is plotted against the number of iterations. It can be seen, that convergence at the beginning of the identification process is very slow. Near the solution point convergence is obtained at a super-linear rate, which is typical for Quasi-Newton methods. This behavior can be regarded as a verification step for the correctness of the sensitivity analysis presented in the previous sections.

In *figure 5* the relative error

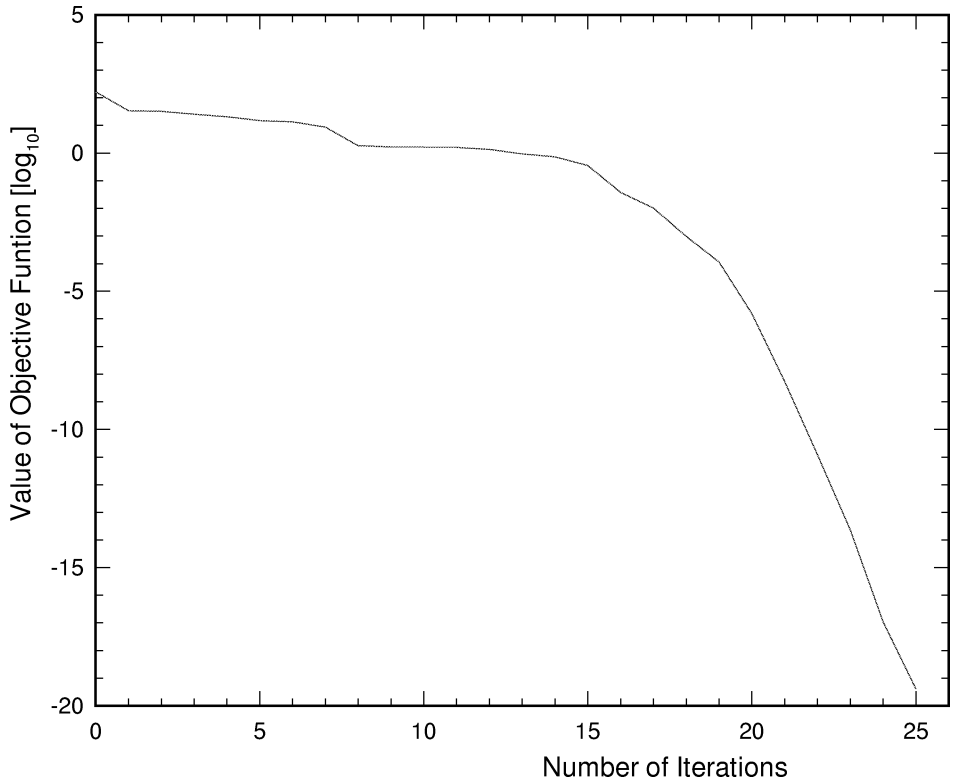

Figure 4. Square panel under tension: Value of the objective function versus number of iterations.

Table III. Square panel under tension: Starting, target and obtained values of the optimization process for the coupled problem.

	starting	target	obtained
α	0.5	0.96	0.96
η	1000.0	350.00	350.00
c	20.0	5.00	5.00

$$e^{(j)}(\kappa) = \frac{\kappa_i^{(j)} - \kappa_i^{\text{final}}}{\kappa_i^{\text{final}}} \tag{45}$$

for each material parameter versus number of iterations is depicted. Clearly the figure illustrates that at the end of the optimization process all parameters obtained their original value κ_i^{final}.

10. Summary

The objective of the work has been the development of a finite element algorithm for parameter identification of material models for a geometrically linear enhanced isotropic damage model based on least-squares minimization. Thereby it is possible to obtain material parameters from in-situ experiments, where quantities such as stress, strain and damage variable are allowed to be non-uniform within the whole volume of the structure. However, the choice of appropriate experimental settings to examine the nonuniform fields is still an unsolved issue.

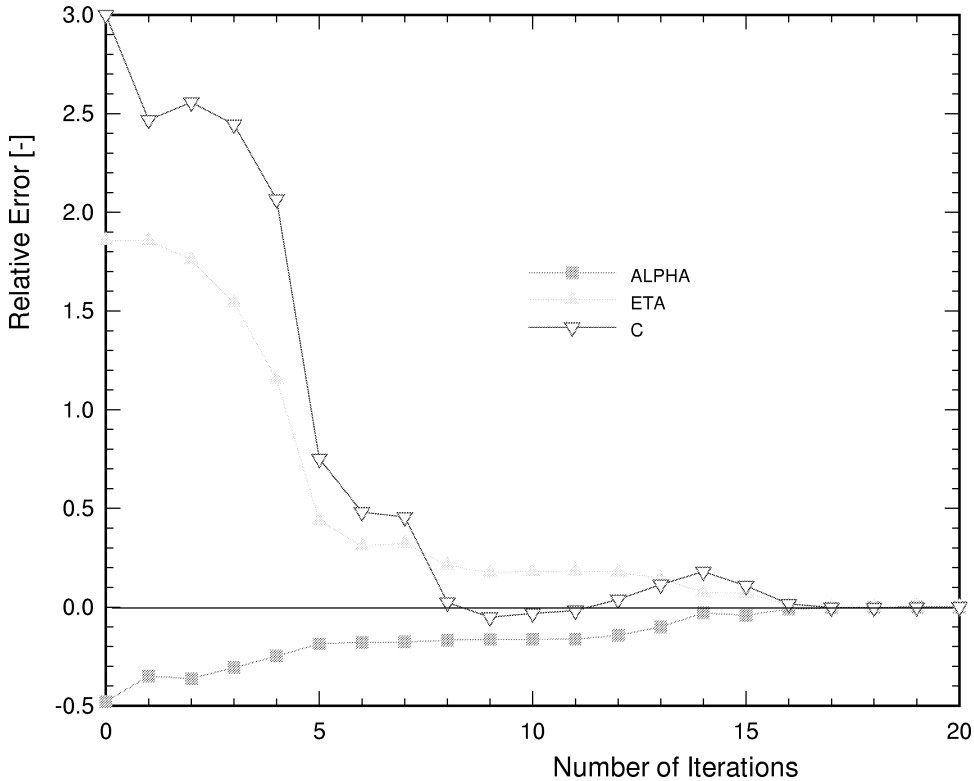

Figure 5. Square panel under tension: Relative error for the material parameters versus number of iterations.

A gradient based optimization algorithm is used for minimizing the least-squares functional for parameter identification, and to this end the associated sensitivity analysis for the coupled weak form consistent with the stress update scheme has been described. On the basis of the proposed algorithm, not only the overall material parameters but also the internal length scale, herein introduced implicitly through the parameter c can be identified from experimental results.

The performance of the algorithm and the correctness of the sensitivity analysis is demonstrated for a square panel under tensile loading, for a specific choice for the geometrically linear gradient enhanced damage model.

In summary this work is considered as a conceptual point of departure for parameter identification of gradient enhanced as well as other nonlocal damage models. Future work should be directed to applications of the algorithm based on real-life experimental data and to investigate the uniqueness of the obtained values. Possible extensions are the incorporation of additional (more realistic) constitutive relations. Furthermore, anisotropic effects or non-homogeneous parameter variations would be a challenging aspect for future work.

References

Andresen K., Dannemeyer S., Friebe H., Mahnken R., Ritter R., Stein E., 1996. Parameteridentifikation für ein plastisches Stoffgesetz mit FE-Methoden und Rasterverfahren. Der Bauingenieur 71, 21–31.

Banks H.T., Kunisch K., 1989. Estimation Techniques for Distributed Parameter Systems. Birkhäuser, Boston.

Bertsekas D.P., 1982. Projected Newton methods for optimization problems with simple constraints. SIAM J. Control. Optim. 20 (2), 221–246.

de Borst R., Geers M.G.D., Kuhl E., Peerlings R.H.J., 1998. Enhanced damage models for concrete fracture. In: de Borst R. et al. (Eds), Computational Modelling of Concrete Structures. Balkema, Rotterdam.

Bui H.D., 1994. Inverse Problems in the Mechanics of Materials, an Introduction. CRC Press, Boca Raton, London.

Bui H.D., Tanaka M. (Eds), 1994. Inverse Problems in Engineering Mechanics. Balkema, Rotterdam.

Dennis J.E., Schnabel R.B., 1983. Numerical Methods for Unconstrained Optimization and Nonlinear Equations. Prentice Hall, New Jersey.

Geers M.G.D., 1997. Experimental analysis and computational modelling of damage and fracture. Ph.D thesis, University of Eindhoven, The Netherlands.

Kuhl E., Ramm E., de Borst R., 1998. An anisotropic gradient damage model for quasi-brittle materials. Comput. Methods Appl. Mech. Engrg., submitted for publication.

Lemaitre J., Chaboche J.L., 1990. Mechanics of Solid Materials. Cambridge University Press, Cambridge.

Luenberger D.G., 1984. Linear and nonlinear programming, 2nd edn. Addison-Wesley, Reading.

Mahnken R., 1992. Duale Verfahren für nichtlineare Optimierungsprobleme in der Strukturmechanik. Dissertation, Forschungs- und Seminarberichte aus dem Bereich der Mechanik der Universität Hannover, F 92/3.

Mahnken R., 1998. Theoretische und numerische Aspekte zur Parameteridentifikation und Modellierung bei metallischen Werkstoffen. Habilitation, Forschungs- und Seminarberichte aus dem Bereich der Mechanik der Universität Hannover, F 98/2.

Mahnken R., Stein E., 1996. Parameter identification of viscoplastic model based on analytical derivatives of a least-squares functional and stability investigations. Int. J. Plast. 12 (4), 451–479.

Mahnken R., Stein E., 1996b. A unified approach for parameter identification of inelastic material models in the frame of the finite element method. Comput. Methods Appl. Mech. Engrg. 136, 225–258.

Mahnken R., Stein E., 1997. Parameter identification for finite deformation elasto-plasticity in principal directions. Comput. Methods Appl. Mech. Engrg. 147, 17–39.

Peerlings R.H.J., de Borst R., Brekelmans W.A.M., de Vree J.H.P., 1996. Gradient-enhanced damage for quasi-brittle materials. Int. J. Numer. Methods Engrg. 39, 3391–3403.

Peerlings R.H.J., de Borst R., Brekelmans W.A.M. and Geers M.G.D., 1998. Gradient enhanced modelling of concrete fracture. Mechanics of Cohesive Frictional Materials 3, 323–342.

Powell M.J.D., 1977. A fast algorithm for nonlinear constrained optimization calculations. In: Watson G.A. (Ed.), Numerical Analysis. Proc. of the Biennial Conference held at Dundee, June 1977, Springer Lecture Notes in Math. 630, Springer, Berlin.

Simo J.C., Ju J.W., 1987. Strain- and stress-based continuum damage models. Int. J. Solids Struct. 23, 821–869.